Fizika Nizkikh Temperatur, 2001, v. 27, No. 1, p. 15–23

Modeling of tunneling spectroscopy in high-T_c superconductors

Yu. M. Shukrinov[1,2], A. Namiranian[1], and A. Najafi[1]

[1] *Institute for Advanced Studies in Basic Sciences, Gava Zang, Zanjan 45195-159, Iran*

[2] *Physical Technical Institute of Tajik Academy of Sciences 299/1 Aini St., Dushanbe, 734063, Tajikistan, C.I.S.*
E-mail: shukr2@iasbs.ac.ir

Received July 11, 2000

The tunneling density of states of high-T_c superconductors is calculated taking into account the tight binding band structure, group velocity, and tunneling directionality for s-wave and d-wave gap symmetry. The characteristic density of states has asymmetry of the quasiparticle peaks, flat s-wave and cusplike d-wave subgap behavior, and an asymmetric background. We consider that the underlying asymmetry of the conductance peaks is primarily due to the features of the quasiparticle energy spectrum, and the d-wave symmetry enhances the degree of asymmetry of the peaks. Increasing the lifetime broadening factor changes the degree of asymmetry of the tunneling conductance peaks and leads to confluence of the quasiparticle and van Hove singularity peaks.

PACS: **74.50.+r**, **74.80.−g**

Introduction

Tunneling measurements on high-T_c superconductors (HTSCs) have revealed a rich variety of properties and characteristics [1–4]. They may be classified according to their low- and high-energy features. With the low-energy features we may attribute: (i) variable subgap shape of the conductance, ranging from a sharp, cusplike, to a flat, BCS-like feature [1]; (ii) voltage and temperature dependence of the quasiparticle conductivity [5,6]; (iii) subgap structure [2]; (iv) zero bias conductance peak (ZBCP) [7]. The high-energy features include: (i) asymmetry of the conductance peaks [1]; (ii) van Hove singularity (VHS); (iii) conductance shape outside of the gap region (background (BG)) and its asymmetry [1]; (iv) dip feature [8]; (v) hump feature [8]. These features are collected schematically in Fig 1. While the tunneling spectroscopy on conventional superconductors allows one to find directly the energy gap of the superconductor, the same measurements in HTSCs are not as easily interpreted. Sometimes the same experiments on the same samples show different results [9] : a cusplike or flat subgap feature; symmetric or asymmetric conductance peaks. Usually the sharpest gap features are obtained when the BG is weakly decreasing. A quantitative measure of it is the ratio of the conductance peak height (PH) to the background conductance: PHB = PH/BG. When the BG conductance is decreasing, the PHB > 2, but when the BG conductance is linearly increasing ($\sim V$), PHB < 2. Kouznetsov and Coffey [10] and Kirtly and Scalapino [11] suggested that the linearly increasing BG arises from inelastic tunneling. As was mentioned in [1], the conductance is dominated by quasiparticle tunneling, and that the effect of Andreev reflection is not significant. A theoretical model for tunneling spectroscopy employing tight-binding band structure, $d_{x^2-y^2}$ gap symmetry,

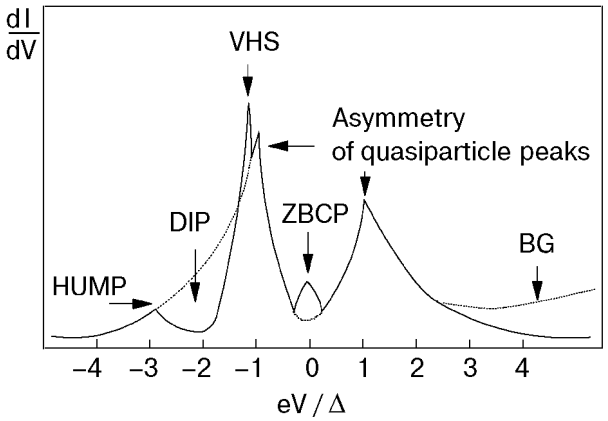

Fig. 1. Schematic dI/dV characteristics of an NIS structure with the main features.

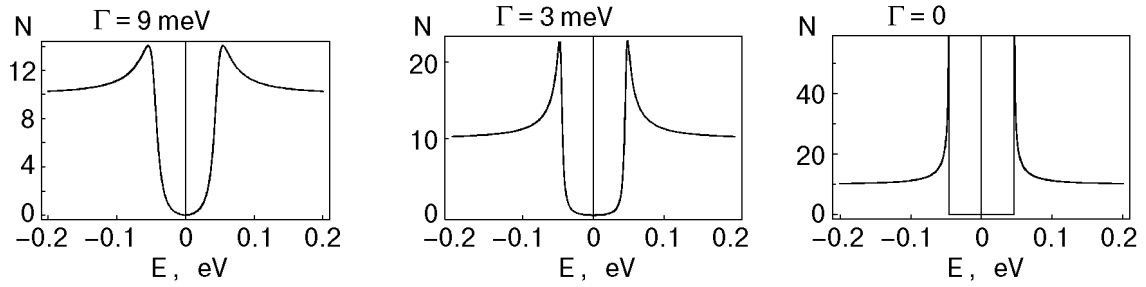

Fig. 2. s-wave DOS at $\Delta = 46$ meV for different values of Γ, calculated by formula (1).

group velocity, and tunneling directionality was studied by Yusof, Zasadzinski, Coffey and Miyahawa [1]. An angle-resolved photoemission spectroscopy (ARPES) band structure specific to optimally-doped BSCCO (Bi-2212) was used to calculate the tunneling density of states for a direct comparison to the experimental tunneling conductance. This model produces an asymmetric, decreasing conductance background, asymmetric conductance peaks, and variable subgap shape, ranging from a sharp, cusplike to a flat, BCS-like feature. A standard technique in analyzing the tunneling conductance is to use a smeared BCS function

$$N(E) = N(0)\,\frac{E - i\Gamma}{\sqrt{(E - i\Gamma)^2 - \Delta^2}}\,, \qquad (1)$$

in which a scattering rate parameter (lifetime broadening factor) Γ is used to take into account any broadening of the gap region in the DOS. Figure 2 shows the DOS calculated by formula (1) at $\Delta = 46$ meV and $\Gamma = 9$ meV (a), $\Gamma = 3$ meV (b), and $\Gamma = 0$ (c). A characteristic feature of the DOS is the flat subgap structure at small Γ. This method cannot explain the asymmetry of the conductance peaks observed in the tunneling experiments.

In the case of d-wave symmetry we have

$$N(E) = N(0)\,\mathrm{Re}\int_0^{2\pi}\frac{d\phi}{2\pi}\,\frac{E - i\Gamma}{[(E - i\Gamma)^2 - \Delta_0^2\cos^2(2\phi)]^{1/2}}\,, \qquad (2)$$

and the DOS calculated by this formula are presented in Fig. 3. The characteristic features of the DOS is the cusplike subgap structure. As was mentioned in [1], this standard technique requires that the comparison be made with normalized tunneling conductance data, and since HTSC tunneling conductance can exhibit a varied and complex background shape, this procedure may «filter out» too much information from the conductance data. An alternative is to simply normalize the data by a constant.

In [8] the tunneling data were first normalized by constructing a «normal state» conductance obtained by fitting the high-bias data to a third-order polynomial. The normalized conductance data were compared to a weighted momentum averaged d-wave DOS:

$$N(E) = \int f(\phi)\,\frac{E - i\Gamma}{[(E - i\Gamma)^2 - \Delta_0^2\cos^2(2\phi)]^{1/2}}\,d\phi\,. \qquad (3)$$

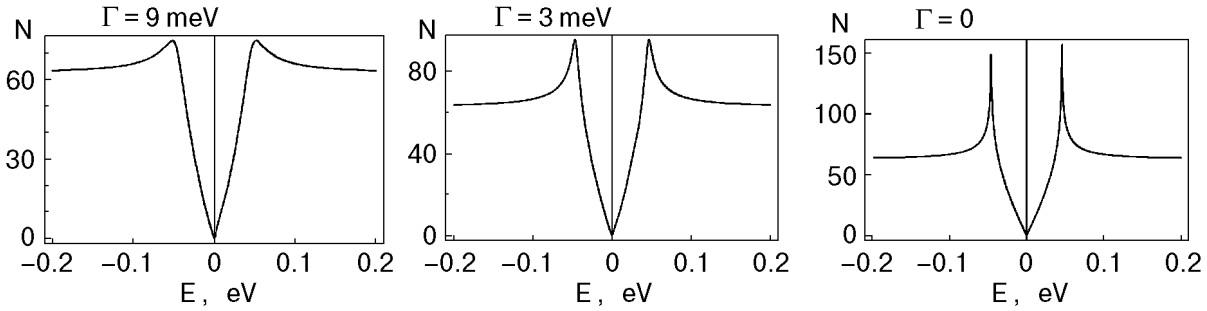

Fig. 3. d-wave DOS at $\Delta = 46$ meV for different values of Γ, calculated by formula (2).

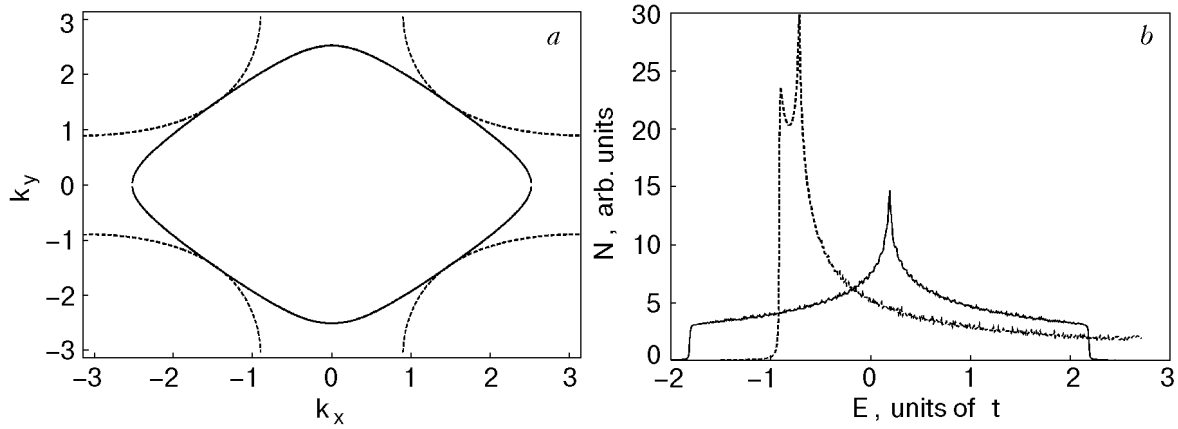

Fig. 4. Fermi surfaces (*a*) and DOS (*b*) for $t' = 0$ (solid lines) and $t' = 0.45t$ (dashed lines) in formula (4) at $\mu/2t = -0.187$ which corresponds hole-doped situation.

Here $f(\phi)$ is an angular weighting function that allows for a better fit with the experimental data in the gap region. A weighting function $f(\phi) = 1 + 0.4 \cos(4\phi)$ was used, which imposes a preferential angular selection of the DOS along the absolute maximum of the d-wave gap and tapers off towards the nodes of the gap. This is a rather weak directional function, since the minimum of $f(0)$ along the nodes of the d-wave gap is still non-negligible [8].

Fedro and Koelling [12] have done a modeling of the normal-state and superconducting DOS of HTSCs, using a tight-binding band structure, including the next-nearest neighbors,

$$\xi_k = -2t\,[\cos(k_x a) + \cos(k_y a)] + \\ + 4t' \cos(k_x a) \cos(k_y a) - \mu\,. \qquad (4)$$

The calculation showed two singularities in the DOS: a van Hove singularity at the center of the energy band due to a saddle point near $(\pi, 0)$ at $t' = 0$, and another at the lower edge of the energy band due to extra flattening out at $(0,0)$. As extended s-wave and d-wave superconducting DOS were considered in case of hole-doped situation ($\mu < 0$) for different hole concentrations. The Fermi surface for $t' = 0$ and $t' = 0.45t$ at the same concentration, corresponding to $\mu/2t = -0.187$, that was used in [12] are presented in Fig. 4,*a*. One must move up from the Fermi surface (set as the zero of energy) to reach the point $(\pi, 0)$ in the case $t' = 0$ and move down in case $t' = 0.45t$. Thus, for $t' = 0$ the Fermi energy lies to the left of the van Hove singularity and will move away from it with increased hole doping, while for $t' = 0.45t$ it lies to the right and will move towards to it with increased hole doping (see Fig. 4,*b*, where the DOS for $t' = 0$ and $t' = 0.45t$ are presented). For calculation of the superconducting DOS Fedro and Koelling used the formula

$$N(E) = \frac{1}{2}\sum_k \left(1 + \frac{\xi_k}{E_k}\right)\delta(E - E_k) + \left(1 - \frac{\xi_k}{E_k}\right)\delta(E + E_k)\,. \qquad (5)$$

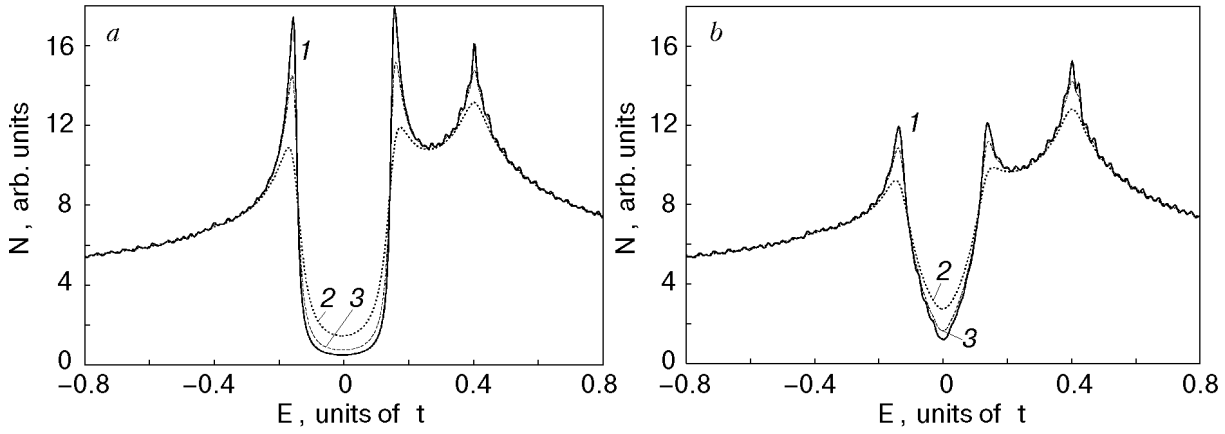

Fig. 5. DOS for $t' = 0$ at different Γ for s-wave symmetry (*a*) and d-wave symmetry (*b*), calculated by formula (5). Curves 1, 2, 3 correspond to the Γ equal 0.07, 0.1, and 0.2, respectively.

This formula is the limit of the expression for the tunneling density of states (6) at $\Gamma = 0$ and $|T_k|^2 = 1$, where T_k is the tunneling matrix element. Figure 5,*a* shows the results of the calculation of the DOS for $t' = 0$ at $\Gamma = 0.07$, 0.1 and 0.2 meV for *s*-wave symmetry, reflecting the results of Fedro and Koelling. Figure 5,*b* shows the same DOS for *d*-wave symmetry. In both cases the Fermi energy (set as the zero of energy) lies to the left of the van Hove singularity. There is asymmetry of the peaks which is more pronounced at large Γ.

Models and methods

In the present paper we use the method for calculation of the DOS in [1]. The tunneling DOS of a superconductor is determined by the imaginary part of the retarded single-particle Green's function,

$$N(E) = -\frac{1}{\pi} \operatorname{Im} \sum_k |T_k|^2 G^R(k, E) . \qquad (6)$$

For the superconducting state

$$G^R(k, E) = \frac{u_k^2}{E - E_k + i\Gamma} + \frac{v_k^2}{E + E_k + i\Gamma} , \qquad (7)$$

where u_k^2 and v_k^2 are the usual coherence factors,

$$u_k^2 = \frac{1}{2}\left(1 + \frac{\xi_k}{E_k}\right), \quad v_k^2 = \frac{1}{2}\left(1 - \frac{\xi_k}{E_k}\right), \qquad (8)$$

and Γ is the quasiparticle lifetime broadening factor. The energy spectrum of quasiparticles in the superconducting state is determined by

$$E_k = \sqrt{|\Delta(k)|^2 + \xi_k^2} \qquad (9)$$

with the effective band structure extracted from ARPES experiments [13],

$$\begin{aligned} \xi_k = C_0 + 0.5C_1 [\cos(k_x a) + \cos(k_y a)] + \\ + C_2 \cos(k_x a) \cos(k_y a) + \\ + 0.5C_3 [\cos(2k_x a) + \cos(2k_y a)] + \\ + 0.5C_4 [\cos(2k_x a) \cos(k_y a) + \\ + \cos(k_x a) \cos(2k_y a)] + \\ + C_5 \cos(2k_x a) \cos(2k_y a). \end{aligned} \qquad (10)$$

Here ξ_k is measured with respect to the Fermi energy ($\xi_k = 0$), and the phenomenological parameters are (in units of eV) $C_0 = 0.1305$, $C_1 =$

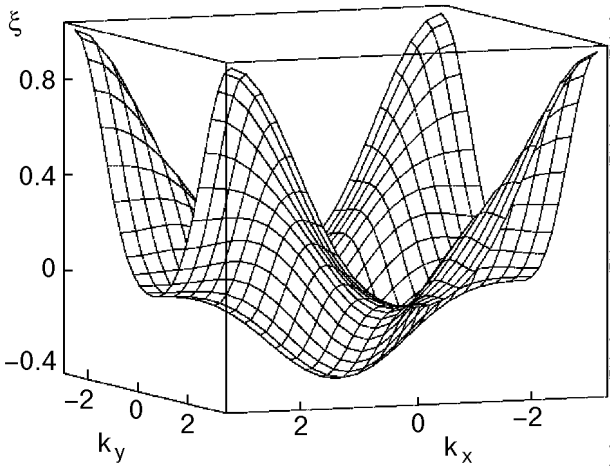

Fig. 6. 3*D* plot of energy spectrum of the normal state, according to formula (9).

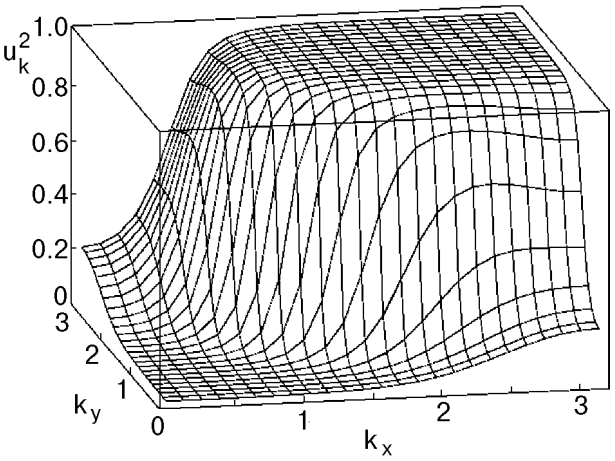

Fig. 7. 3*D* plot of the coherence factor u_k^2 according to formula (8).

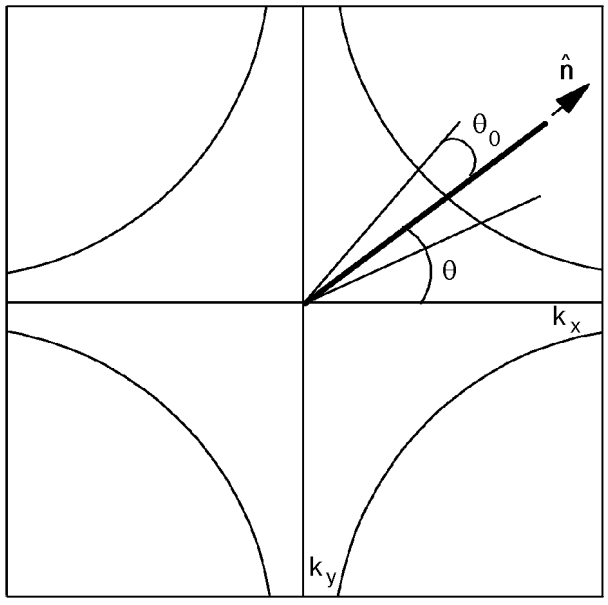

Fig. 8. Fermi surface corresponding to the $\xi_k = 0$ in formula (10). The heavy straight line shows the line of directional tunneling, and the lighter lines show the angular spread θ_0 .

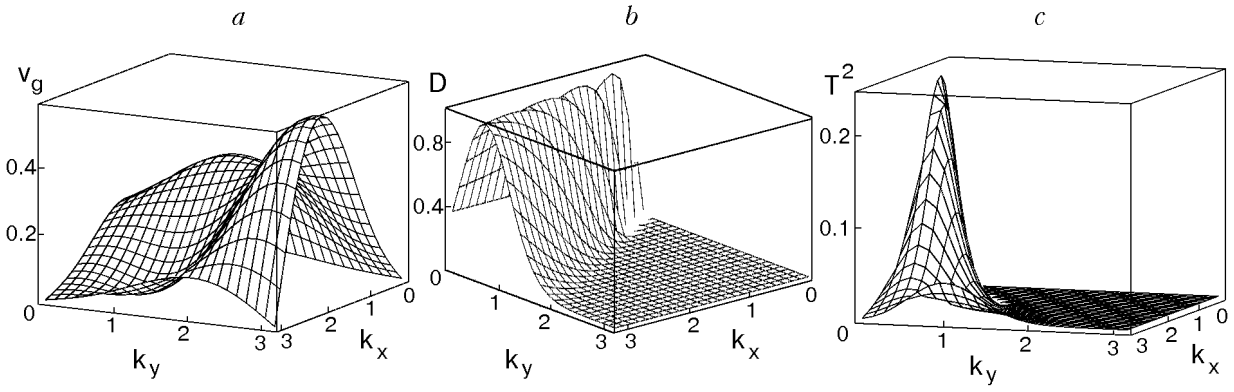

Fig. 9. 3*D* plot of the group-velocity function (*a*), the directionality function (*b*) and the tunneling matrix element (*c*) according to formulas (11), (12), and (13), respectively.

$= -0.5951$, $C_2 = 0.1636$, $C_3 = -0.0519$, $C_4 = -0.1117$, and $C_5 = 0.0510$.

Figure 6 shows the three-dimensional image of function (10). There are a saddle point at $(\pi,0)$ and a flattening out of the energy band at $(0,0)$, which lead to the van Hove singularities in the DOS. The three-dimensional graph of the coherence factor u_k^2 is shown in Fig. 7.

Since quasiparticles with momentum perpendicular to the barrier interface have the highest probability of tunneling, the tunneling matrix element $|T_k|^2$ reveals a need for factors of directionality $D(k)$ and group velocity $v_g(k)$ [1]. The group velocity factor is defined by

$$v_g(k) = |\nabla_k \xi_k \cdot \hat{\mathbf{n}}| = \left| \frac{\partial \xi_k}{\partial k_x} \cos\theta + \frac{\partial \xi_k}{\partial k_y} \sin\theta \right| , \tag{11}$$

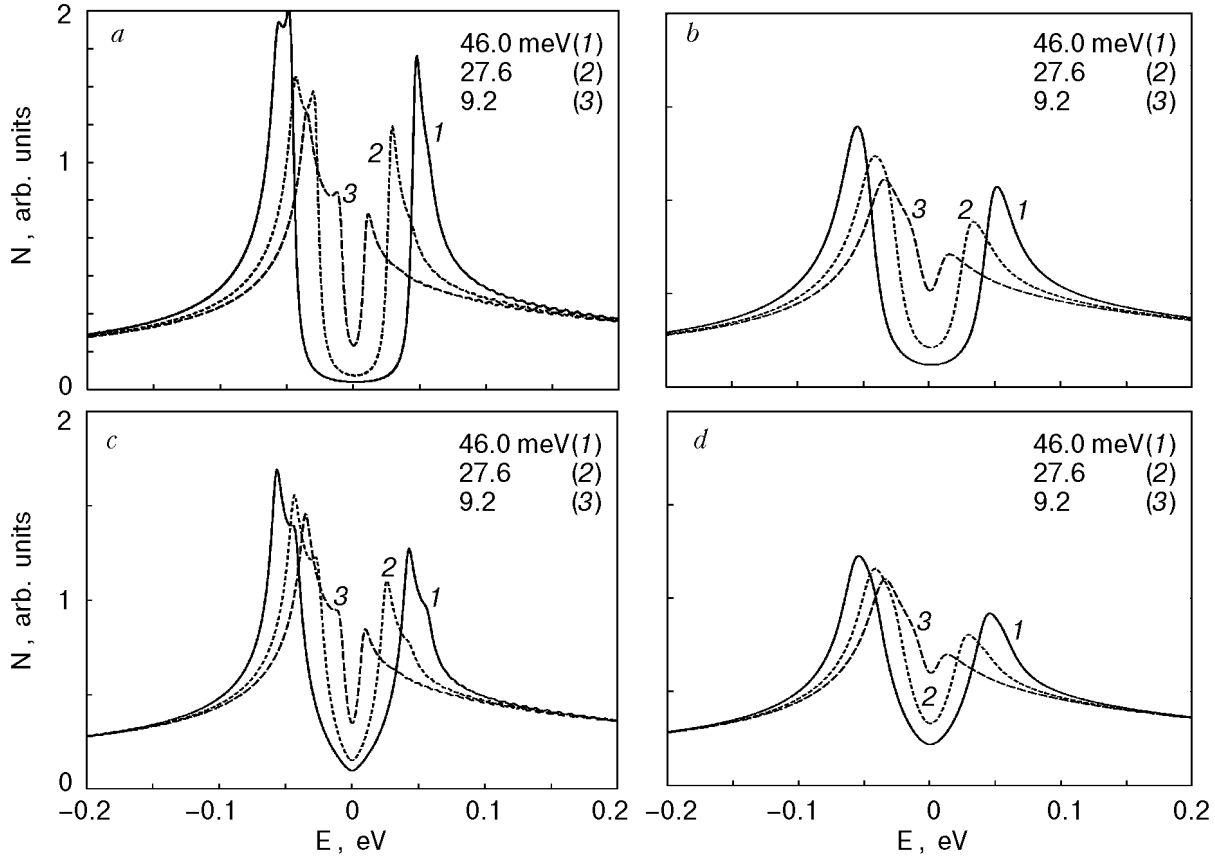

Fig. 10. The changing of DOS with energy gap Δ_0 for *s*- (*a*,*b*) and *d*-wave (*c*,*d*) symmetry at $\Gamma = 3$ meV (*a*,*c*) and $\Gamma = 9$ meV (*b*,*d*) without effects of directionality and group velocity.

where the unit vector **n** defines the tunneling direction as shown in Fig. 8, which is perpendicular to the plane of the junction.

The directionality function $D(k)$ is defined by

$$D(k) = \exp\left[-\frac{k^2 - (\mathbf{k}\cdot\hat{\mathbf{n}})^2}{(\mathbf{k}\cdot\hat{\mathbf{n}})^2\theta_0^2}\right]. \qquad (12)$$

Here θ_0 defines the angular spread of the quasiparticle momentum with non-negligible tunneling probability with respect to $\hat{\mathbf{n}}$. The tunneling matrix element $|T_k|^2$ is written as

$$|T_k|^2 = v_g(k)\, D(k)\ . \qquad (13)$$

The three-dimensional graphs of the group velocity $v_g(k)$, directionality $D(k)$, and tunneling matrix element $|T_k|^2$ functions are shown in Fig. 9.

Results and discussions

Different factors may lead to the changing of the energy gap Δ_0 in HTSC. In particular, strong effects are caused by nonmagnetic impurities [14]. In superconductors with d-wave symmetry the nonmagnetic impurities destroy the superconductivity very efficiently. The possibility of destruction of Cooper pairs by impurities leads to their finite lifetime. If the state with the quasiparticle is not stationary state, it must attenuate with time due to transitions to other states. The corresponding wave function has the form $\exp(-i\xi(p)t/\hbar - \Gamma t/\hbar)$, where Γ is proportional to the probability of the transitions to the other states. It may be interpreted as an imaginary addition $-i\Gamma$ to the energy of the quasiparticle. The relation between Γ and lifetime of quasiparticle τ_s is $\Gamma = \hbar/\tau_s$. Hence, the impurities lead to changing of Δ_0 , and we may do modeling of the influence of impurities on tunneling conductance by numerical calculations of the DOS $N(E)$ considering different values of Δ_0 in formula (6). Here we present the results of a calculation of $N(E)$ at $\Delta_0 = \alpha\Delta_{00}$, where $\alpha = 0.2,\ 0.4,\ 0.6,\ 0.8,\ 1$ and $\Delta_{00} = 46$ meV.

The peculiarities of the quasiparticle energy spectrum (10) play an essential role in explanation of the conductance features. Here, based on the numerical calculations of the DOS, we consider that the underlying asymmetry of the conductance peaks is primarily due to the features of the quasiparticle energy spectrum. The d-wave gap symmetry simply enhances the degree of the asymmetry of the peaks. Thus last is also changed by varying the tunneling direction.

Figure 10 shows the results of the numerical calculations of the DOS at $\Gamma_0 = 3$ meV (a,c) and $\Gamma_0 = 9$ meV (b,d) without the group velocity and directionality effects for both s-wave (a,b) and d-wave (c,d) gap symmetry, respectively for different values of the energy gap Δ_0 . We have decreased the energy gap Δ_0 , starting from $\Delta_0 = 46$ meV. For clarity we present only three characteristic curves, which correspond to $\alpha\Delta_0$ with $\alpha = 1,\ 0.6$, and 0.2. We exclude the group velocity and directionality effects to demonstrate that they are not responsible for the asymmetry of the peaks.

There is asymmetry of the quasiparticle peak heights for both s- and d-wave symmetry. Thus the origin of the asymmetry of the peaks is not due to d-wave symmetry of the energy gap of the HTSC. There is a flatter subgap behavior of the DOS in the case of s-wave symmetry in comparison with the d-wave case. The increase of the lifetime broadening factor Γ leads to enhancement of the asymmetry of the peaks. There are van Hove singularities (VHSs) in the DOS at small Γ. Increasing Γ leads to confluence of the quasiparticle and VHS peaks and this results to enhancement asymmetry of the DOS peaks due to the saddle point in the energy spectrum (10) at $(\pi,\ 0)$. Also note the asymmetry of the background for both s- and d-wave gap symmetry.

Figure 11 shows the Δ_0 dependence of the DOS, taking into account the group-velocity and directionality effects at $\Gamma = 3$ meV (a,c) and $\Gamma = 9$ meV (b,d) for s-wave (a,b) and d-wave (c,d) gap symmetry. As in [1] we have taken $\theta = 0.25$ and $\theta_0 = 0.1$.

There is also asymmetry of the quasiparticle peaks, similar to the s- and d-wave cases. But in the d-wave case the asymmetry is stronger than in the s-wave case. The group-velocity and directionality effects lead to disappearance of the VHSs in the DOS. Increasing Γ enhances the asymmetry of the quasiparticle peak. The strongest effect of the energy band structure on the DOS occurs along the k_x axis due to the van Hove singularity at $(\pi,\ 0)$.

Figure 12 demonstrates this effect. We have presented the DOS at different θ at $\Gamma = 3$ meV (a,c) and $\Gamma = 9$ meV (b,d) for both s-wave (a,b) and d-wave (c,d) gap symmetry. In the case of s symmetry the position of the quasiparticle peaks is constant except in the direction along k_x $(\theta = 0)$. We note the strong asymmetry of the peaks in this case.

In the case of d-wave symmetry we have practically the same behavior around the k_x direction as for the s wave, but the energy gap is changed due to the θ dependence of Δ_0 and, correspondingly, the quasiparticle peaks are shifted to zero energy.

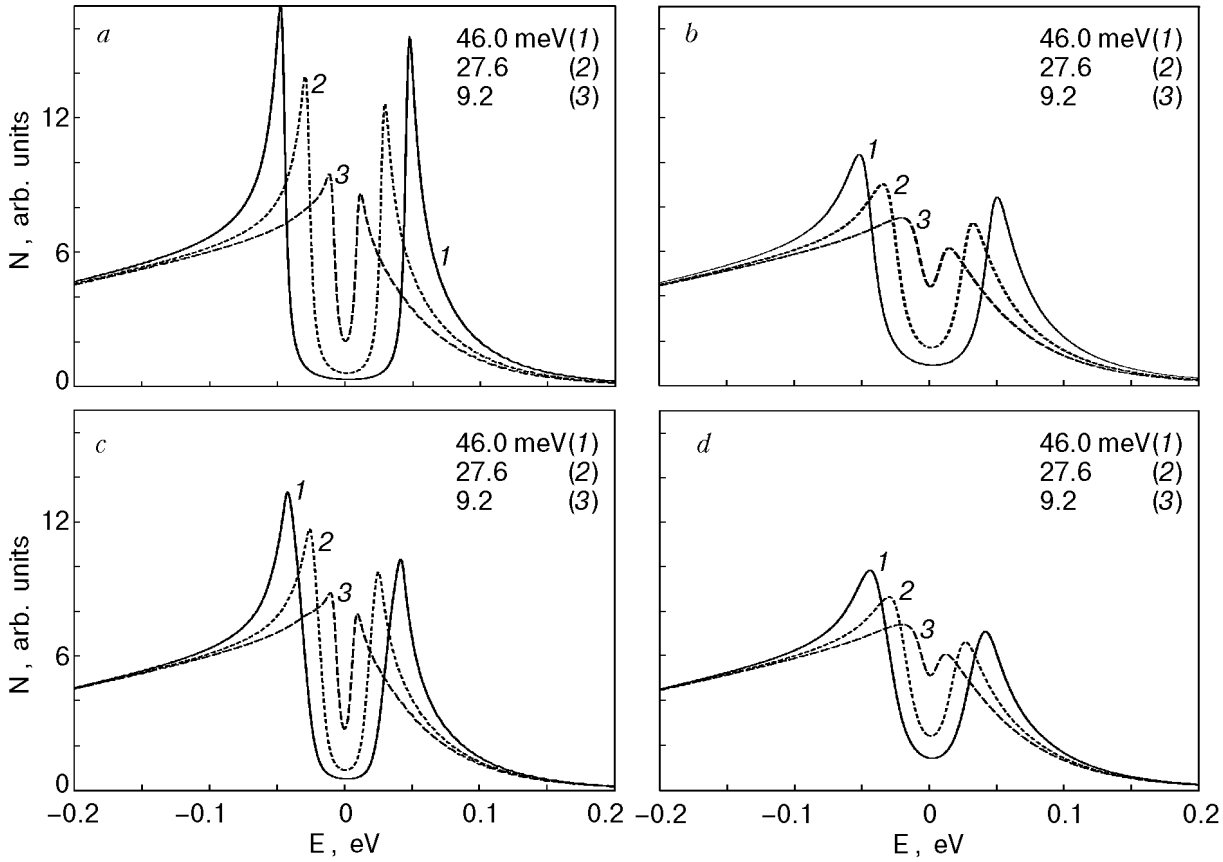

Fig. 11. The change of DOS with energy gap Δ_0 for *s*- wave (*a*,*b*) and *d*-wave (*c*,*d*) gap symmetry at $\Gamma = 3$ meV (*a*,*c*) and $\Gamma = 9$ meV (*b*,*d*) with the effects of directionality and group velocity.

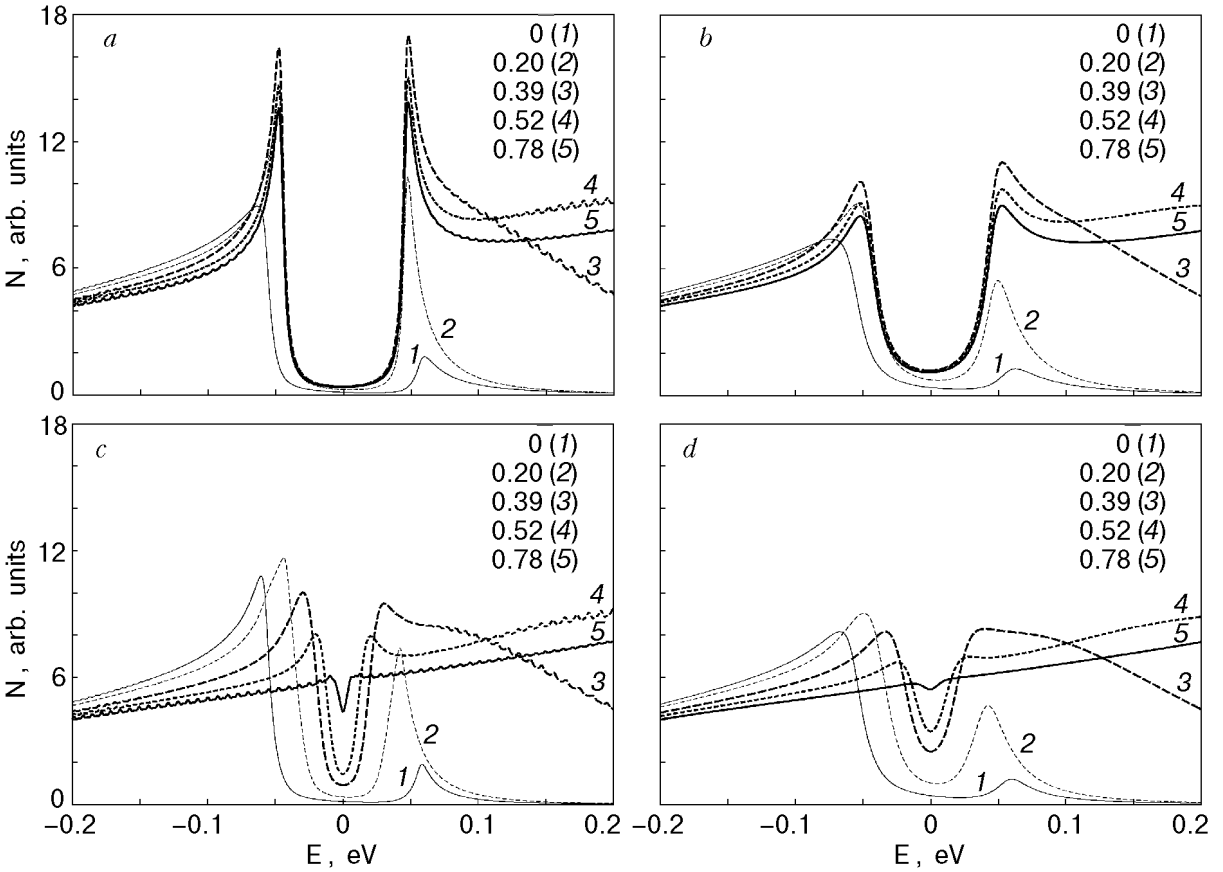

Fig. 12. Effects of directionality on the DOS for *s*-wave (*a*,*b*) and *d*-wave gap symmetry at $\Gamma = 3$ meV (*a*,*c*) and $\Gamma = 9$ nothing meV (*b*,*d*).

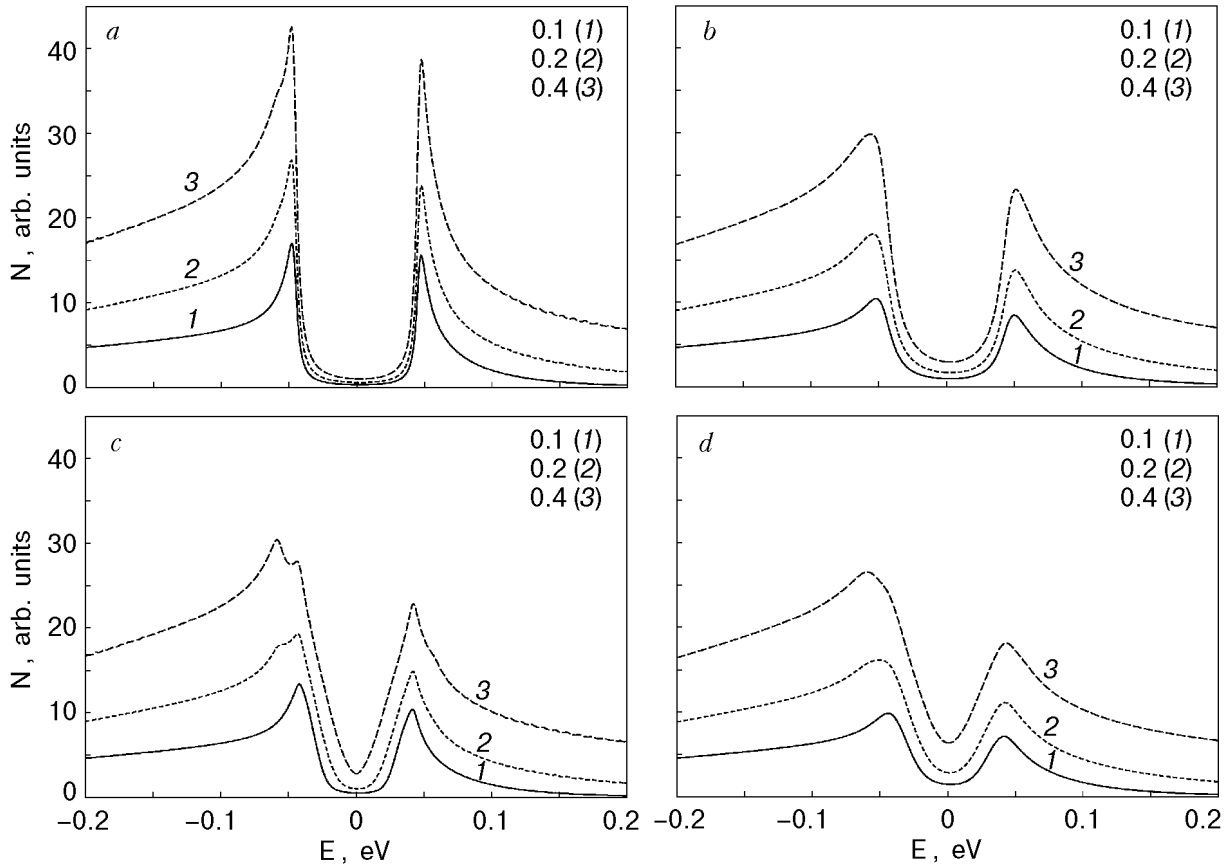

Fig. 13. Numerical calculation of the quasiparticle DOS with s-wave (a,b) and d-wave (c,d) gap symmetry at $\Gamma = 3$ meV (a,c) and $\Gamma = 9$ meV (b,d) for different spreads θ_0 .

Figure 13 shows the change of the DOS with θ_0 at $\Gamma = 3$ meV (a,c) and $\Gamma = 9$ meV (b,d) for both s-wave (a,b) and d-wave (c,d) gap symmetry. Increasing θ_0 brings into play the states close to $(\pi, 0)$. It is reflected as an appearance of a van Hove singularity in both the case of s-wave and d-wave gap symmetry at small Γ. The VHS is more pronounced in the d-wave case in comparison with the s-wave symmetry. Increasing Γ leads to confluence of the quasiparticle and VHS peaks.

We consider that the absence of the VHS peak on the experimental dI/dV characteristics is indicative of a rather large lifetime broadening factor Γ in that HTSC material.

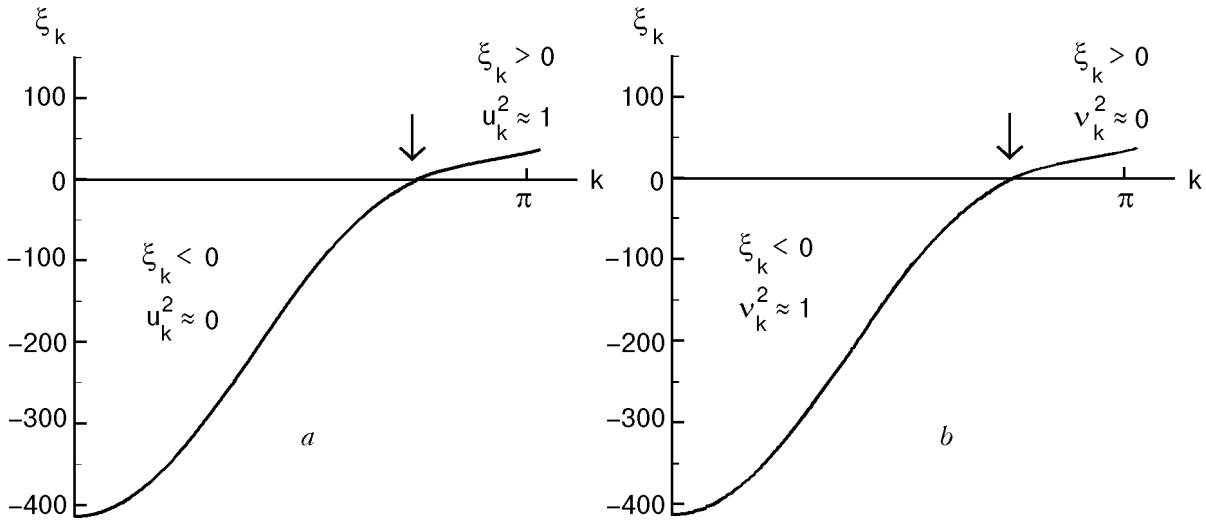

Fig. 14. ARPES energy spectrum along $\theta = 0.25$. The values of the coherence factors correspond to $E > 0$ (a) and $E < 0$ (b).

The origin of the asymmetry of the peaks in the tunneling DOS was studied in [1] by considering the role of the tunneling matrix element $|T_k|^2$ in the clean limit $\Gamma = 0$, where formula (5) was used for the calculation of $N(E)$.

We repeat the explanation of the paper [1] because we believe that the conclusion as to the origin of the peak asymmetry must be different. At $E > 0$ (positive bias voltages) the first term of (5) contributes to $N(E)$ because of $\delta(E_k - E)$. In this case, as one can see from Figs. 7, 9,*c*, and 14,*a*, $|T_k|^2$ selects only a relatively short region of states in k-space in which $u_k^2 > 0$. These are the states with $\xi_k > 0$ (above the FS). For the majority of states integrated over at $E < 0$ (negative bias voltages, see again Figs. 7 and 9,*c*) the second term of (5) contributes to the DOS because of $\delta(E_k + E)$. In this case, as one can see from Figs. 7, 9,*c*, and 14,*b*, $|T_k|^2$ selects out a large region of k states where $v_k^2 > 0$, in fact, equal to one. These states are below the Fermi surface, where $\xi_k < 0$. The overall effect then is to have a large negative bias conductance compared to the positive one. This is true for both *s*- and *d*-wave symmetry. Hence, the underlying asymmetry of the conductance peaks is primarily due to the band structure ξ_k, and *d*-wave symmetry simply enhances the degree of asymmetry of the peaks. So, the asymmetry of the peaks, which exists for both *s*-wave and *d*-wave symmetry, is sensitive to the band structure ξ_k .

In summary, by changing of the energy gap Δ_0 in HTSC one may model the influence of nonmagnetic impurities on the DOS. We consider that the asymmetry of the quasiparticle peaks is due to the specific features of the energy spectrum of HTSC and that the *d*-wave gap symmetry only enhances the peaks asymmetry.

The absence of the VHS peak on the experimental dI/dV charactristics means the large enough lifetime broadening factor Γ in HTSC.

Acknowledgement

We thank Y. Sobouti, M. R. H. Khajehpour and also Yu. A. Kolesnichenko for useful discussions.

1. Z. Yusof, J. F. Zasadzinski, L. Coffey, and N. Miyakawa, *Phys. Rev.* **B58**, 514 (1998).
2. K. Schlenga, R. Kleiner, G. Hechtfischer, M. Moessle, D. Schmitt, Paul Mueller, Ch. Helm, Ch Preis, F. Forsthofer, J. Keller, M. Veith, and E. Steinbess, *Phys. Rev.* **B57**, 14518 (1998).
3. Yu. M. Shukrinov, Kh. Nasrulloev, Kh. Mirzoaminov, and I. Sarhadov, *Appl. Superconductivity* **2**, 741 (1994).
4. Yu. M. Shukrinov, A. Stetsenko, Kh. Nasrulloev, and M. Kohandel, *IEEE Transaction on Appl. Supercond.* **8**, 142 (1998).
5. Yu. I. Latyshev, T. Yamashita, L. N. Bulaevskii, M. J. Graf, A. V. Balatsky, and M. P. Maley, *Cond.-mat./9903256*.
6. Yu. Shukrinov, P. Seidel, and J. Scherbel, *Quasiparticle current in the intrinsic Josephson junctions in TBCCO* (to be publ).
7. A. M. Cucolo, *Physica* **C305**, 85 (1998).
8. L. Ozyuzer, Z. Yusof, J. Zasadzinski, T. Li, T. Hinks, and K. E. Gray, *Cond.-mat./9905370*.
9. Y. DeVilde , N. Migakawa, P. Iavarone, L. Ozyuzer, J. F. Zasadzinski, P. Romano, D. G. Hinks, C. Kendziora, G. W. Grabtree, and K. E. Gray, *Phys. Rev. Lett.* **80**, 153 (1998).
10. K. Kouznetsov and L. Coffey, *Phys. Rev.* **B54**, 3617 (1996).
11. J. R. Kirtley and D. J. Scalapino, *Phys. Rev. Lett.* **65**, 798 (1990).
12. A. J. Fedro and D. D. Koelling, *Phys. Rev.* **B47**, 14342 (1993).
13. M. R. Norman, M. Randeria, H. Ding, and J. C. Campuzano, *Phys. Rev.* **B52**, 615 (1995).
14. A. A. Abrikosov, *Physica* **C244**, 243 (1995).